



Trade Science Inc.

Materials Science

An Indian Journal

Full Paper

MSAIJ, 9(10), 2013 [372-377]

Sol-gel quaternary bioactive glass scaffold for bone repair

Enobong Reginald Essien¹, Luqman A.Adams^{2*}, Rafiu O.Shaibu²¹Department of Chemical Sciences, Bells University of Technology, (NIGERIA)²Department of Chemistry, Faculty of Science, University of Lagos, (NIGERIA)

E-mail: ladams@unilag.edu.ng

ABSTRACT

Bioactive glass of the quaternary system; $\text{SiO}_2\text{-Na}_2\text{O-CaO-P}_2\text{O}_5$ similar to 45S5 Bioglass® was prepared using sol-gel chemistry from fused silica sand. The monolith was sintered at 950 °C before subjecting to immersion in simulated body fluid (SBF). The sintered monolith and immersion specimen were characterised by scanning electron microscopy (SEM), energy dispersive X-ray analysis (EDX) and Fourier transform infrared spectroscopy (FTIR). The density of the as-sintered glass was 1.056 g/cm³ and porosity 61%. Immersion study of the glass monolith in simulated body fluid confirmed steady change in pH of the SBF solution, increase in Ca, P and C on the surface of the monolith, with corresponding decrease in Si attributed to the formation of carbonated hydroxyapatite (HCA). The compositionally controlled glass material prepared shows promise as a candidate scaffold material for bone tissue engineering.

© 2013 Trade Science Inc. - INDIA

KEYWORDS

Simulated body fluid;
Sol-gel;
Bioactive glass;
Carbonated hydroxyapatite;
Scaffold material.

INTRODUCTION

Human tissue and organ failure caused by defects, injuries, diseases or any other types of damage impact substantially on the health and quality of life of the population and as such, impose huge financial burden on the economy. Among these, musculoskeletal conditions occur frequently as a major reparative problem in reconstructive surgery. One of the surgical strategies pursued to remedy this problem include utilization of autografts or allografts^[1]. While the use of autograft material is the preferred technique, there are limitations such as donor site morbidity, limited donor bone supply, anatomical and structural problems, and elevated levels of resorption during healing^[2]. Allografts have the

disadvantage of eliciting immunological response due to genetic differences and the risk of inducing transmissible diseases^[3,4]. Therefore, considerable attention has been directed towards regeneration of damaged bones in vivo and in vitro using bioactive glasses and engineered biomaterials^[5,6]. Bioceramic calcium phosphates such as hydroxyapatite (HA), tricalcium phosphate (TCP), biphasic calcium phosphate (BCP) and related composites of bioactive inorganic materials with biodegradable polymers^[7-9] are some of the most promising materials for application in bone tissue engineering.

Bioactive inorganic materials are biocompatible reacting with physiological fluids forming tenacious bonds to bone through the formation of bone-like HA layers. Several authors have proposed a three-step mecha-

nism of HCA formation when a bioactive glass with composition in the system $\text{SiO}_2\text{-Na}_2\text{O-CaO-P}_2\text{O}_5$ comes into contact with physiological fluids to include; ion exchange, dissolution and precipitation^[10-12]. This phenomenon facilitates strong interfacial fixation of bone tissue with the material surface without eliciting adverse immunological responses^[13,14]. For example, silicate bioactive glasses such as 45S5 Bioglass®^[14] (composition in mol %: SiO_2 (46.1); Na_2O (24.4); CaO (26.9); P_2O_5 (2.6)) induces the release and exchange of critical concentrations of soluble Si, Ca, P and Na ions, which lead to favourable intracellular and extracellular responses promoting rapid bone formation^[15,16].

Sol-gel derived bioactive glasses^[17-21] have been reported to show better activity over the melt-derived glass material^[22,23]. Also, sodium containing bioactive glasses have some advantages over their non-sodium bioglass, for example addition of Na_2O or K_2O lowers the temperature during processing of melt-derived bioactive glasses. Furthermore, inclusion of Na makes the final material more soluble in aqueous media^[24,25] and enhances its mechanical strength due to the crystallization of sodium calcium silicate phases which are biodegradable^[26]. Additionally, the sol-gel processing method facilitates high intrinsic surface area^[26,27] resulting in high reactivity in physiological fluids.

Most sol-gel reactions to give bioactive glasses utilize as precursors silicon alkoxides like trimethyl orthosilicate (TMOS) and tetraethyl orthosilicate (TEOS) as starting materials. These alkoxides are not only expensive, but also toxic on inhalation^[29-31]. In continuation of our interest in the synthesis of bioactive glass scaffolds suitable for bone tissue repair, we report herein the preparation of bioactive glass in the quaternary system containing $\text{SiO}_2\text{-CaO-Na}_2\text{O-P}_2\text{O}_5$ from inexpensive and readily available silica rich sand as a precursor via the sol-gel process.

EXPERIMENTAL

Materials

The sand used as starting material was obtained from Ifo in Ogun State, Nigeria having the composition shown in TABLE 1. Analytical grade reagents including; $\text{Ca}(\text{NO}_3)_2 \cdot 4\text{H}_2\text{O}$ (Loba Chemicals, 98 %),

$\text{NaH}_2\text{PO}_4 \cdot 2\text{H}_2\text{O}$ (Kermel, 99 %), HNO_3 , HCl (Riedel-deHaen, 60%), H_3PO_4 , NaCl , NaHCO_3 , KCl , $\text{K}_2\text{HPO}_4 \cdot 3\text{H}_2\text{O}$, $\text{MgCl}_2 \cdot 6\text{H}_2\text{O}$, CaCl_2 , and trishydroxymethyl aminomethane [Tris-buffer, $(\text{CH}_2\text{OH})_3\text{CNH}_2$] were used as appropriate to prepare either the bioglass or SBF solution respectively.

Preparation of sodium metasilicate from sand

The silica sand sized by passing through sieves ranged between 159-595 μm was washed to free it from clay and other impurities before being oven-dried at 120 °C. Soda ash was added to the sand to obtain the ratio $\text{Na}_2\text{O} : \text{SiO}_2$ of 1: 2 in the final product. The mixture after thorough mixing was fused in a furnace at 1300 °C for 1 h to form water glass, sodium metasilicate melt.

Preparation of bioactive glass

To prepare the bioactive glass with composition (mol %); 31.39 SiO_2 : 28.70 Na_2O : 36.86 CaO : 3.05 P_2O_5 , the sodium metasilicate melt (water glass) was added slowly while using a magnetic stirrer to 0.05M HNO_3 . The mixture was stirred for 1 h for complete hydrolysis, thereafter under stirring conditions H_3PO_4 , $\text{NaH}_2\text{PO}_4 \cdot 2\text{H}_2\text{O}$ and $\text{Ca}(\text{NO}_3)_2 \cdot 4\text{H}_2\text{O}$ were added slowly in that order. Each reagent was added in a molar ratio of 1:20 of water and allowed reaction time of 45 minutes before adding the next reagent. After the last addition, the mixture was stirred further for 1 h before pouring the resulting sol into teflon moulds and kept at room temperature for 72 h for gelation. Thereafter, the gel was maintained at; i. 70 °C/72 h, 130 °C/42 h, ii. 700 °C/2 h, and iii. 950 °C/3 h to age, dry, stabilize and sinter respectively. The heating and cooling rate were maintained at 5 °C/min.

Characterization

The density of the bioactive glass ρ_{glass} was determined from the mass and dimensions of the sintered material. The porosity P was calculated as follows;

$$P = (1 - \rho_{\text{glass}} / \rho_{\text{solid}}) \times 100 \quad (1)$$

where density $\rho_{\text{solid}} = 2.7 \text{ g/cm}^3$ of 45S5 Bioglass®^[26]. Furthermore, microstructure of the glass was characterized before and after immersion in simulated body fluid (SBF) using EVO/MAIO scanning electron microscope (SEM) equipped with energy dispersive X-

Full Paper

ray analyzer (EDX). The sample was carbon-coated and observed at an accelerating voltage of 15kV. Fourier transform infrared (FTIR, Shimadzu 8400S), with the wave number range of 4000-400 cm^{-1} employing KBr pellets operating in a reflectance mode with a 4cm^{-1} resolution was used to investigate the nature of bonds present in the glass network.

Bioactivity test

Assessment of bioactivity was carried out using the standard in vitro procedure described by Kokubo *et al.*^[27]. SBF was prepared using analytical grade reagents; NaCl, NaHCO_3 , KCl, $\text{K}_2\text{HPO}_4 \cdot 3\text{H}_2\text{O}$, $\text{MgCl}_2 \cdot 6\text{H}_2\text{O}$, CaCl_2 , trishydroxymethyl aminomethane [Tris-buffer, $(\text{CH}_2\text{OH})_3\text{CNH}_2$], and 1 M HCl with ions concentrations shown in TABLE 2. Monolith glass samples were immersed in acellular SBF at concentration of 0.01 g/ml in clean plastic bottles, which had previously been washed using HCl and deionised water. The bottles were placed inside an incubator at a controlled temperature of 36.5 °C and pH was maintained at 7.4. without refreshing the SBF solution for a maximum of 14 days and the pH recorded daily for the first 9 days using a pH meter (Hanna, HI96107). The samples were extracted from the SBF solution after 7 and 14 days, rinsed with deionised water and left to dry at ambient temperature in a desiccator. The samples were thereafter investigated for formation of apatite layer on the glass surface by SEM/EDX and FTIR.

RESULTS AND DISCUSSION

Densification, bulk density and porosity

Chemical analysis of the sand used in this study is shown in TABLE 1. The result reveals that the sand is rich in silica, approximately 98%. Most of the other metal oxides components in the sand occur in minor amount making this sand satisfactory for the desired purpose. Water glass was obtained using standard procedure. The quaternary bioactive glass of desired composition was obtained as described. The density of the as-sintered glass was 1.056 g/cm^3 while porosity obtained by applying Eq. (1) was 61 %, indicating that only partial densification occurred after heating the glass at 950 °C for 3 h. This result is quantitatively similar to Chen *et al.*^[32] who showed that complete densification

of Bioglass® construct may be obtained after sintering above 950 °C. Implicitly, extensive densification leads to hardening of a material by strengthening the pore struts and overall reduction in porosity. Significant densification of the glass may cause full crystallization for which a bioactive glass may revert into an inert material^[33]. It is also imperative to note that insufficient densification may occur at low temperature which can lead to a very fragile scaffold containing loosely packed particles. Consequently, it is desirable that the material should be sintered at a temperature where crystallization does not occur to a great extent to maintain bioactivity of the glass and should be highly porous, both which are ideal for tissue engineering scaffold.

TABLE 1 : Composition of silica sand.

Element	SiO_2	Fe_2O_3	MgO	Al_2O_3	K_2O	Na_2O	CaO
(%)mass	98	0.97	0.046	0.53	0.35	0.043	0.061

SEM/EDX characterisation of bioactive glass before and after immersion in SBF

SEM micrograph of the sol-gel glass after sintering at 950 °C is shown in Figure 1(a). The glass material shows heterogeneous surfaces of flaky particles with little crystallinity and some porous structure. After 7 days immersion in SBF solution, the surface is transformed into agglomerated balls of HA growth in Figure 1(b) and 1(c). The composition of the surface as shown by EDX indicates that the concentration of sodium in the bioactive glass decreases based on the dissolution theory in physiological fluids^[11,28], while concentrations of Ca and P increase due to the formation of HA^[34-36]. After 14 days in SBF solution, the HA particles appear coarser shown in Figure 1(d) with many small protuberances growing out from the apatite layer. The reaction process proposed for the formation of HA on the surface of a glass sample immersed in SBF^[37] involves; exchange of the network modifier calcium with protons, dissolution of soluble silica at the glass solution interface, condensation and re-polymerization of a SiO_2 -rich layer on the surface, finally migration of Ca^{2+} and PO_4^{3-} ions to the surface to form a $\text{CaO-P}_2\text{O}_5$ -rich film.

Furthermore, from the EDX (Figure 1(d) inset), it is evident that the composition of Si on the surface has reduced considerably, while Ca, P and C have all increased. The low detection by EDX of Si as shown in TABLE 3 is due to the apatite cover on the bioactive

glass. Furthermore, the variation in both Ca, P and C with increased immersion time in SBF is due to chemisorption to explain the HA dissolution/redeposition theory^[37-39], TABLE 3.

TABLE 2 : Ion concentrations (mM) in human plasma in comparison with SBF.

Ion	Na ⁺	K ⁺	Mg ²⁺	Ca ²⁺	Cl ⁻	HCO ₃ ⁻	HPO ₄ ²⁻	SO ₄ ²⁻
SBF	142.0	5.0	1.5	2.5	147.8	4.2	1.0	0.5
Human Plasma	142.0	5.0	1.5	2.5	103.0	27.0	1.0	0.5

pH changes during immersion in SBF

Changes in pH of the SBF solution after immersing the bioactive glass for the first 9 days is shown in Figure 2. The pH of the solution increased sharply for

the first two days reaching a value of 8.4 compared with the initial pH of 7.4, then remains constant until the 4th day. This is due to the fast release of Na⁺ and Ca²⁺ ions into the surrounding solution through exchange with H⁺ or H₃O⁺ ions^[40]. With the H⁺ ions being replaced by cations, there is a concomitant increase in hydroxyl concentration of the solution that result in attack on the silica glass network and formation of silanols at the glass solution interface. After day 4 the pH increases more gradually because some of the released calcium ions are used to form CaO–P₂O₅-rich film, decreasing the Ca release kinetics. With prolonged immersion, the pH reaches a saturated state (pH = 8.7).

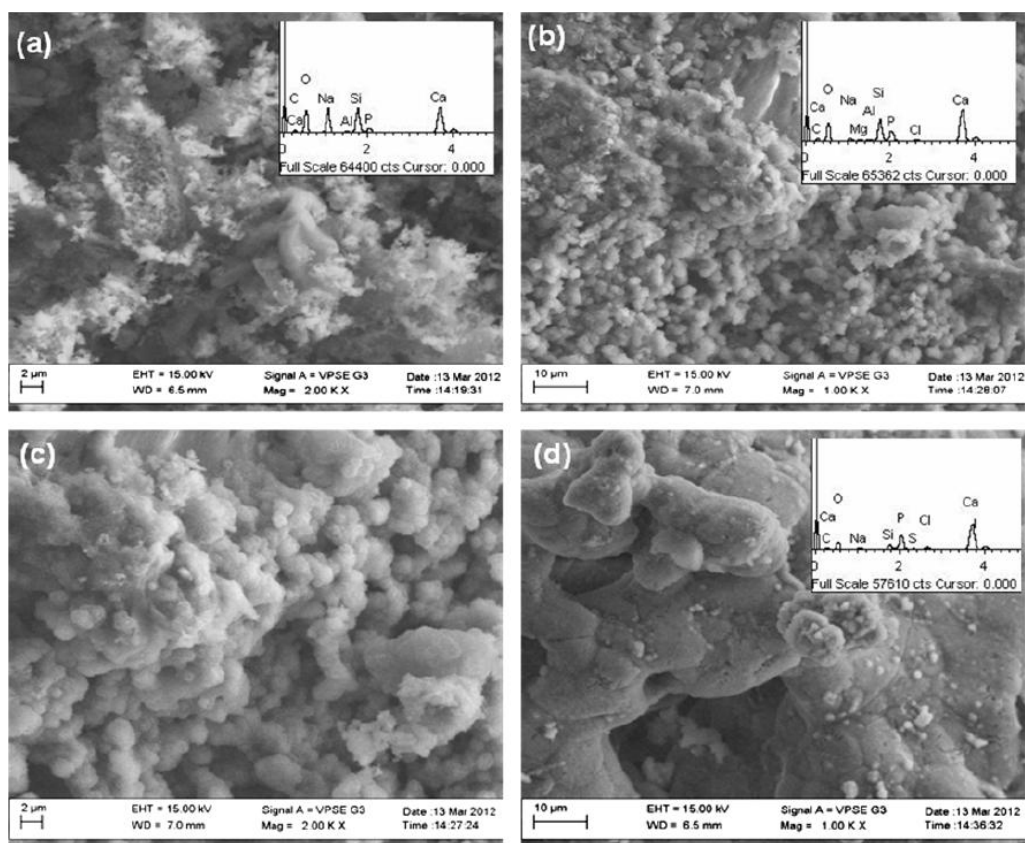


Figure 1 : SEM micrographs with EDX insets of the bioactive glass surface at (a) 0 day, (b and c) 7 days at different magnifications and (d) 14 days showing growth of HA and increase in P with increasing immersion time in SBF.

FTIR evaluation of bioactivity of the glass

Figure 3 shows the FTIR spectra of samples immersed in SBF solution for 0, 7 and 14 days respectively. As observed, the spectrum of the parent glass before immersion reveals bands at 1119, 1038, 964, 930, 901, 797, 681, 641, 617, 567, 511 and 475 cm⁻¹. The bands 1119 and 1038 cm⁻¹ are associated with

Si–O–Si and P–O vibrational modes^[37]; 900-964 cm⁻¹ are related to Si–O non-bridging oxygen bonds (NBO). The bands at 797 and 475 cm⁻¹ are attributed to Si–O–Si bending vibrations. The peak at 612 cm⁻¹ can be assigned to the presence of crystalline phase in the sample^[41]. After soaking for 7 days only two bands appear in the region 1100-900 cm⁻¹; a sharp band at

Full Paper

1082 and a shoulder at 959 cm^{-1} suggesting the disruption of the NBO bonds due to leaching of Ca and dissolution of soluble silica at the glass interface during the period of immersion in SBF solution^[42]. Several new peaks emerge at 1427, 872 cm^{-1} , which can be attributed to the presence of CO_3^{2-} ^[43], and the peak at 573 cm^{-1} is assigned to P–O bend in amorphous calcium phosphate. This suggests the onset of incorporation of CO_3^{2-} into HA. After 14 days of immersion, the bands between 950–1120 cm^{-1} increase in number which may be due to re-polymerization of SiO_2 to form silica rich-layer on the glass surface and incorporation of Ca^{2+} . Additionally, the CO_3^{2-} band becomes broader and develops a second band at 1470, while the peak at 573 cm^{-1} splits into two sharp modes at 604 and 554 cm^{-1} , which are characteristic of apatite crystalline phase^[35], indicating that HCA now dominates the apatite phase.

TABLE 3 : Composition (in atomic %) of the bioactive glass surface before and after immersion in SBF measured by EDX.

Element (%)	Immersion time (days)		
	0	7	14
Ca	7.90	10.58	14.45
P	1.31	3.33	7.20
Si	6.68	5.58	2.10
C	13.62	15.28	16.62
Na	12.25	1.58	1.83
Cl	-	0.34	1.13
S	-	0.08	0.33
Mg	-	0.49	0.25
Al	0.28	0.16	-
I	-	-	0.18

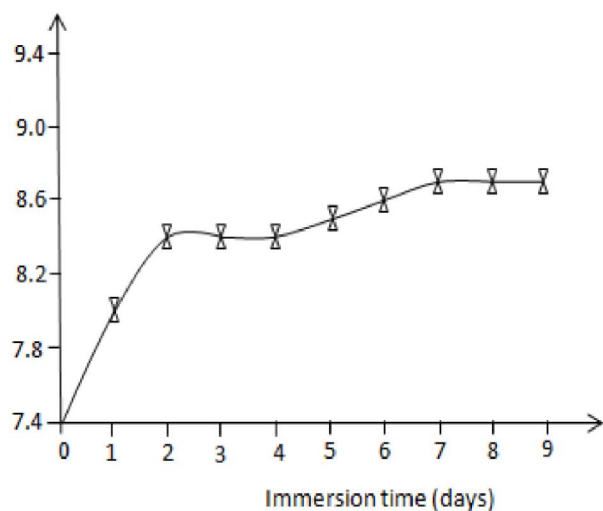


Figure 2 : Variation in pH of bioactive glass immersion in SBF solution with time at initial pH = 7.4.

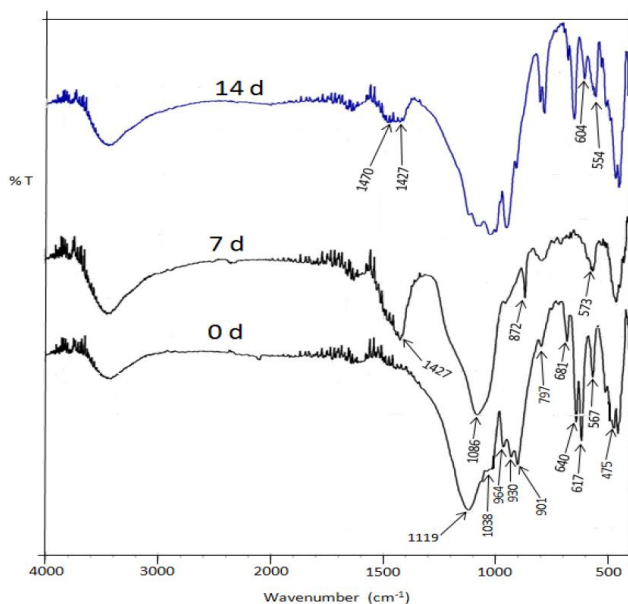


Figure 3 : FTIR spectra of the bioactive glass immersed in SBF solution for 0-14 days.

CONCLUSION

Bioactive glass material of the quaternary system $\text{SiO}_2\text{--Na}_2\text{O--CaO--P}_2\text{O}_5$ has been obtained by the sol-gel technique using sand obtained from Ifo in Nigeria to prepare the water glass precursor. The monolith obtained was sintered at 950 $^\circ\text{C}$ in order to attain reasonable crystallinity without achieving full densification to ensure the material is also resorbable in physiological fluids. Evidence from this study shows that pH of the SBF changes gradually from 7.4, reaching a value of 8.7 after 14 days, which will imply a controlled rate of degradation leading to HCA formation that will facilitate osteoconductivity. Finally, the low cost precursor used and the low-temperature sol-gel processing conditions could serve as a novel inexpensive approach to prepare quaternary bioactive glasses with potentials for rapid commercialization in bone repair therapy.

REFERENCES

- [1] C.Ohtsuki, M.Kamitakahara, T.Miyazaki; *J.R.Soc.Interface*, **6**, S349 (2009).
- [2] C.G.Finkemeier; *J.Bone Joint Surg.Am.*, **84**, 454 (2002).
- [3] I.Binderman, N.Fin; *Bone substitutes-organic, inorganic, and polymeric: Cell material interactions*, In T.Yamamuro, L.L.Hench, J.Wilson, Boca Raton

- (Eds); Handbook of Bioactive Biomaterials, CRC Press, 45-61 (1990).
- [4] C.R.Perry; Clin.Orthop., **360**, 71 (1999).
- [5] M.N.Rahaman, D.E.Day, B.S.Bal, Q.Fu, S.B.Jung, L.F.Bonewald, A.P.Tomsia; Acta Biomater., **7**, 2355 (2011).
- [6] D.Williams; Mater.Today, **7**, 24 (2004).
- [7] S.M.Best, A.E.Porter, E.S.Thian, J.Huang; J.Eur.Ceram.Soc., **28**, 1319 (2008).
- [8] V.Guarino, F.Causa, L.Ambrosio; Expert Rev.Med.Devices, **4**, 405 (2007).
- [9] D.W.Hutmacher, J.T.Schantz, C.X.F.Lam, K.C.Tan, T.C.Lim; J.Tissue Eng.Regen.Med., **1**, 245 (2007).
- [10] V.Banchet, E.Jallot, J.Michel, L.Wortham, D.Laurent-Maquin, G.Balossier; Surf.Interface Anal., **36**, 658 (2004).
- [11] L.L.Hench, R.J.Splinter, W.C.Allen, T.K.Greenlee Jr.; J.Biomed.Mater.Res., **2**, 117 (1971).
- [12] T.Kokubo; Anales de Quimica, **93**, S49 (1997).
- [13] M.E.Felipe, P.F.Andrade, A.B.Novaes, M.F.Grisi, S.L.Souza, M.Taba, D.B.Palioto; J.Periodontol., **80**, 808 (2009).
- [14] L.C.Gerhardt, A.R.Boccaccini; Materials, **3**, 3867 (2010).
- [15] L.L.Hench; J.Mater.Sci.Mater.Med., **17**, 967 (2006).
- [16] J.R.Jones; J.Eur.Ceram.Soc., **29**, 1275 (2009).
- [17] A.Balamurugan, G.Sockalingum, J.Michel, J.Fauré, V.Banchet, L.Wortham, S.Bouthors, D.Laurent-Maquin, G.Balossier; Mater.Lett., **60**, 3752 (2006).
- [18] Z.Gou, J.Chang, W.Zhai; Eur.Ceram.Soc., **25**, 1507 (2005).
- [19] J.R.Jones, L.M.Ehrenfried, L.L.Hench; Biomaterials, **27**, 964 (2006).
- [20] W.Liang, M.N.Rahaman, D.E.Day, N.W.Marion, G.C.Riley, J.J.Mao; J.Non-Cryst.Solids, **354**, 1690 (2008).
- [21] W.Xia, J.Chang; J.Non-Cryst.Solids, **354**, 1338 (2008).
- [22] A.Lucas-Girot, F.Z.Mezahi, M.Mami, H.Oudadesse, A.Harabi, M.L.Floch; J.Non-Cryst.Solids, **357**, 3322 (2011).
- [23] P.Sepulveda, J.R.Jones, L.L.Hench; J.Biomed. Mater.Res., **61**, 301 (2002).
- [24] D.Arcos, D.C.Greenspan, M.Vallet-Regi; J.Biomed.Mater.Res., **65**, 344 (2003).
- [25] M.Vallet-Regi, F.Balas; Open Biomed.Eng.J., **2**, 1 (2008).
- [26] W.Cao, L.L.Hench; Ceram.Int., **22**, 493 (1996).
- [27] L.L.Hench, J.Wilson; Science, **226**, 630 (1984).
- [28] T.Kokubo, H.Takadama; Biomaterials, **27**, 2907 (2006).
- [29] M.Crisan, M.Raileanu, S.Preda, M.Zaharescu, A.M.Valean, E.J.Popovici, V.S.Teodorescu, V.Matejec, J.Mrazek; J.of Optoelectronics & Adv.Mater., **8**, 815 (2006).
- [30] Z.Li, B.Hou, Y.Xu, D.Wu, Y.Sun, W.Hu, W.Deng, F.Deng; J.Solid State Chem., **178**, 1395 (2005).
- [31] E.Pabon, J.Retuert, R.Quijada, A.Zarate; Microp.Mesopor.Mater., **67**, 195 (2004).
- [32] Q.Chen, I.D.Thompson, A.R.Boccaccini; Biomaterials, **27**, 2414 (2006).
- [33] P.Li, F.Zhang, T.Kokubo; J.Mater.Sci.Med., **3**, 452 (1992).
- [34] T.Kokubo, S.Ito, T.Huang, T.Hayashi, S.Sakka, T.Kitsugi; J.Biomed.Mater.Res., **24**, 331 (1990).
- [35] J.M.Oliveira, R.N.Correia, M.H.Fernandes; Biomaterials, **23**, 371 (2002).
- [36] M.Vallet-Regi, M.Pérez-Pariente, I.Izquierdo-Barba, A.Salinas; Chem.Mater., **12**, 3770 (2000).
- [37] O.Peitl, E.D.Zanotto, L.L.Hench; J.Non-Cryst.Solids, **292**, 115 (2001).
- [38] P.Li, K.de Groot, T.Kokubo; J.Sol-Gel Sci.Technol., **7**, 27 (1996).
- [39] T.Kokubo H.-M.Kim, M.Kawashita; Biomaterials, **24**, 2161 (2003).
- [40] J.P.Zhong, G.P.La Torre; Bioceramics, **7**, 61 (1994).
- [41] L.Lefebvre, J.Chevalier, L.Gremillard, R.Zenati, G.Thollet, D.Bernache-Assolant, A.Govin; Acta Mater., **55**, 3305 (2007).
- [42] M.M.Pereira, A.E.Clark, L.L.Hench; J.Biomed.Mater.Res., **28**, 693 (1994).
- [43] M.Mami, A.Lucas-Girot, H.Oudadesse, R.Dorbez-Sridi, F.Mezahi, E.Dietrich; Appl.Surf.Sci., **254**, 7386 (2008).